Study on linear conjugated combination of Zernike modes

Saisai Niu (钮赛赛)[1*], Jianxin Shen (沈建新)[1], Wenhe Liao (廖文和)[1,2], Chun Liang (梁 春)[1], and Yunhai Zhang (张运海)[3]

[1] *College of Mechanical and Electrical Engineering, Nanjing University of Aeronautics and Astronautics, Nanjing 210016, China*

[2] *Nanjing University of Science and Technology, Nanjing 210094, China*

[3] *Suzhou Institute of Biomedical Engineering and Technology, Chinese Academy of Sciences, Suzhou 215163, China*

[*] *Corresponding author: nssycit@163.com*

Received July 14, 2012; accepted September 26, 2012; posted online January 21, 2013

We present linear conjugated combined aberration modes with a concentric pupil diameter of 4 mm. The combinations are according to the coupling relationship between Zernike modes over the concentric circle domain within the unit circle and the root mean square decreasing amplitude ratio of the corresponding aberration modes in the concentric pupil, in which the reconstruction pupil diameter is 6 mm. Each combined mode shares the characters of 2 radial orders apart, the same azimuth frequency, the same coefficient sign, and the prescribed amount, such as ($C_2^0 = 0.7\lambda$, $C_4^0 = 0.3\lambda$), ($C_3^{-3} = 0.8\lambda$, $C_5^{-3} = 0.3\lambda$), and so on. We also analyze the influence of the combined modes on optical quality. Simulations and experiments show improvement after combination; they also indicate that the influence of conjugated combination on optical quality has compensation and not superposition.

OCIS codes: 220.1000, 110.1080.

doi: 10.3788/COL201311.022201.

The existence of human eye aberrations reduces human visual performance and limits the subtle observation of the internal organizational structure of the human eye. Adaptive optics (AO) technology can solve the problems caused by such human eye aberrations[1]. Thanks to the rapid development of AO technology and aberration correction theory, research on human eye aberration has intensified in recent years[2]. Normalized Zernike polynomial expansion is the most commonly used method for describing human eye aberration, and has become the standard for reporting human eye optical aberrations[3]. The advantage of this method is that the value of each item polynomial coefficient represents the wavefront aberration root mean square (RMS).

Complete and real-time compensations of human eye aberration in space and time domains are the main problems that AO technology aims to solve[4,5]. For this reason, the study of the human eye Zernike aberration characteristics has gradually become the new research focus in recent years[6], especially aimed at the interaction between the Zernike aberrations. Thibos *et al*. identified the significant correlations of human eye Zernike aberration by statistical approach and suggested that these correlations may have an effect on optical quality[7]. Several studies have demonstrated the interaction between the low and high order aberrations. Applegate *et al*., for example, studied the interaction between the 2nd and the 4th order Zernike aberrations based on the visual acuity measurement experiment; their results indicate that acuity varies significantly depending on the aberration type and amount of the combined aberrations[8]. Based on the objective evaluation metrics of human eye optical quality, Fang *et al*. analyzed the compensation relationship between defocus (Z_2^0) and spherical aberration (Z_4^0), as well as the influence of aberration combination on optical quality within the same total aberration RMS, obtaining a similar conclusion as that of a previous work[9,10]. The abovementioned typical combination effects on the symmetrical Zernike terms have also been described in Refs. [11, 12]. McLellan *et al*. investigated the effects on the modulation transfer function (MTF) of the interactions among the higher order aberrations and those amongthe chromatic and monochromatic aberrations[13,14]. Gracia *et al*. have

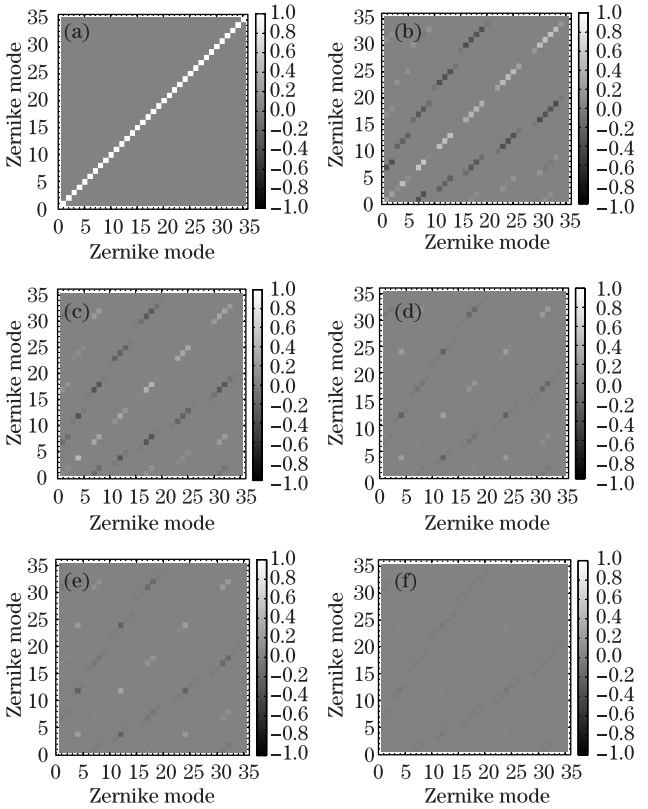

Fig. 1. Correlation matrices of the Zernike modes over different concentric circles. (a) ω=1, (b) ω=0.9, (c) ω=0.7, (d) ω=0.5, (e) ω=0.3, and (f) ω=0.1.

studied the potential interactive effects of astigmatism (Z_2^{-2} and Z_2^2) and coma (Z_3^{-1} and Z_3^1) using computer simulations of optical quality and measurement of visual acuity in subjects under controlled aberration. Their results indicate that optical/visual quality improved in the presence of astigmatism and coma[15,16].

However, most previous studies do not provide a comprehensive combination of Zernike modes. In this letter, we present the linear conjugated combination of Zernike modes based on the comprehensive correlation analysis of Zernike modes in different concentric pupil regions. Simulations and experiments are presented to verify the performance of the proposed combined modes. Results show that the favorable interaction of the conjugated combination of Zernike modes improve optical quality compared with only using the either one mode, especially in the inner wavefront reconstruction region where the improvement is more significant. Such results also demonstrate that cancelling the either one mode in the wavefront aberration Zernike polynomial expansion does not necessarily produce better optical quality. Consequently, conjugated combination can be widely used in aberration correction for AO, because higher order aberration can be compensated by adding the lower order aberration. Therefore, the correction capability of the corrector is improved and a new aberration correction theory can be introduced. The conjugated combination of Zernike modes also has a theoretical significance for personalized refractive surgery in vision science.

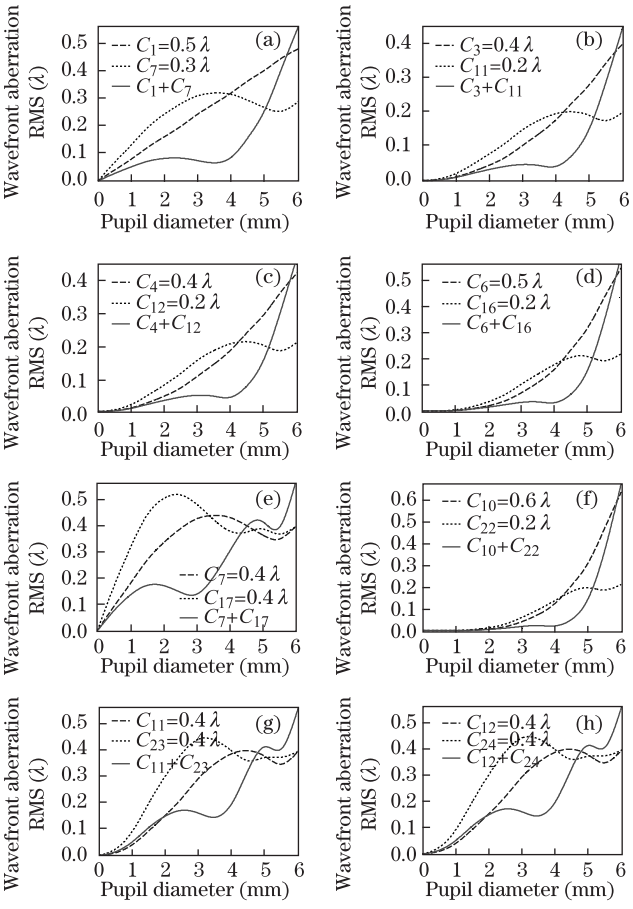

Fig. 2. Wavefront aberration RMS values before and after mode combination with different concentric pupil diameters.

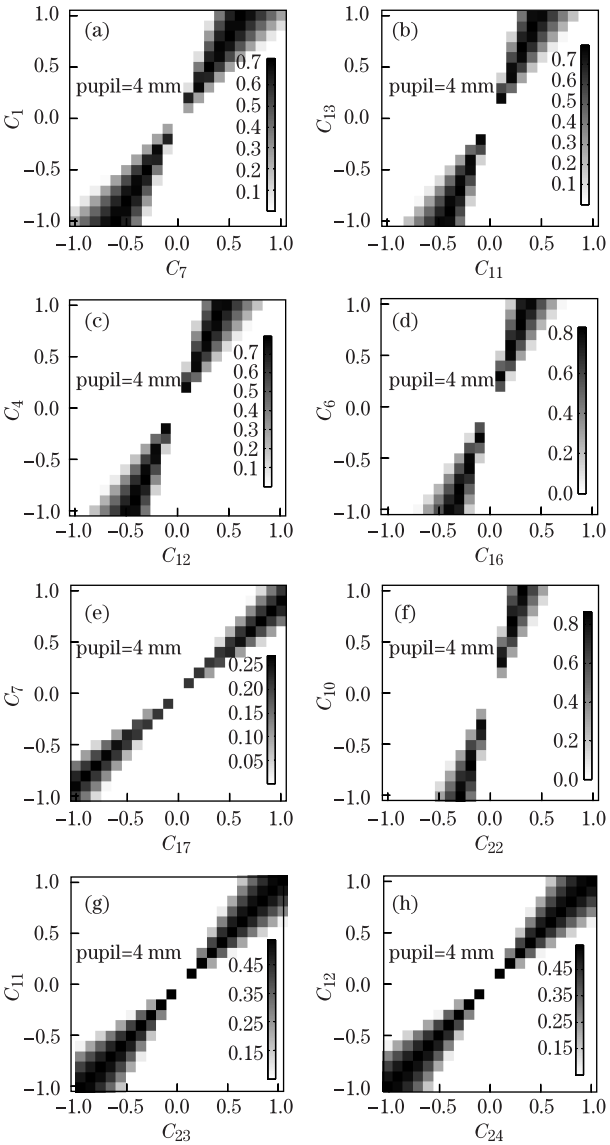

Fig. 3. RMS decreasing amplitude ration R^p_{RMS} matrix with different combination coefficients of the Zernike combined modes.

The Zernike polynomials are usually defined in polar coordinates (ρ, θ), where ρ is the radial coordinate ranging from 0 to 1, and θ is the azimuthal component ranging from 0 to 2π. Each item of the polynomials goes by the name of basis function or wavefront mode, which is referred to as a mode. The wavefront aberration can be expressed as follows:

$$\varphi(\rho,\theta) = \sum_{i=0}^{\infty} C_i N_i Z_i(\rho,\theta), \tag{1}$$

where C_i, N_i, and $Z_i(\rho,\theta)$ are the polynomial coefficient, normalization factor, and polynomial expression of the ith Zernike mode, respectively. The total wavefront aberration RMS can be expressed as follows:

$$\mathrm{RMS} = \sqrt{\sum_{i=0}^{\infty}(C_i)^2}. \tag{2}$$

Any two Zernike modes (except the piston mode) with

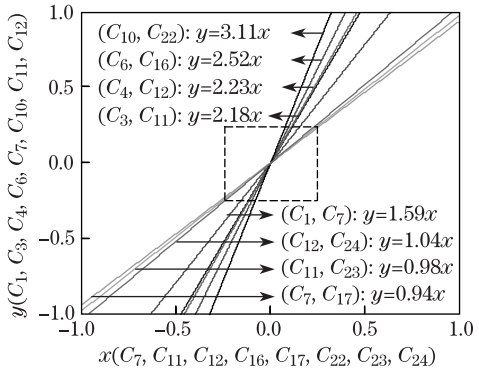

Fig. 4. Optimal linear relationships of the conjugated combination coefficients for maximum $R^p_{\rm RMS}$ values between the combined Zernike modes.

normalization factor have the same standard orthogonality over the unit circle domain ($0 \leqslant \theta \leqslant 2\pi, 0 \leqslant \rho \leqslant 1$) with continuous points, which is given as follows:

$$\frac{1}{\pi}\int_0^1\int_0^{2\pi} N_i\cdot Z_i(\rho,\theta)\cdot N_i\cdot Z_j(\rho,\theta)\rho{\rm d}\rho{\rm d}\theta=\begin{cases}0, {\rm if}(i\neq j)\\ 1, {\rm if}(i=j)\end{cases}. \tag{3}$$

However, over the concentric circle domain within the unit circle ($0 \leqslant \theta \leqslant 2\pi, 0 \leqslant \rho \leqslant \omega, 0 < \omega \leqslant 1$), the orthogonality between each mode is no longer valid. In order to describe the correlation between each Zernike mode of this case, we define the correlation matrix of Zernike modes as P using the following equation:

$$P_{i,j} = \frac{1}{\pi}\int_0^w\int_0^{2\pi} N_i\cdot Z_i(\rho,\theta)\cdot N_i\cdot Z_j(\rho,\theta)\rho{\rm d}\rho{\rm d}\theta, \tag{4}$$

where $P_{i,j}$ is the correlation coefficient of the ith and jth Zernike modes. When $P_{i,j} = 0$, it indicates uncorrelated Zernike modes, whereas $P_{i,j} > 0$ and $P_{i,j} < 0$ indicate positive and negative correlation, respectively. The correlation matrices of Zernike modes when ω equals different values are shown in Fig.1 in the form of gray-scale images.

When $\omega = 1$, which stands for the unit circle domain, it means that the value of the correlation matrix diagonal element is 1 and that of the remaining element is 0 (i.e., the unit orthogonality described in Eq. (3)) (Fig. 1). When ω equals other values ($0 < \omega < 1$), which stand for the concentric circle within the unit circle domain, the values of the correlation matrices of some non-diagonal elements are not 0, indicating that there is coupling relationship between these modes. These coupling phenomena appear with certain regularity, that is, as the ω value decreases, the nonzero value of the correlation matrix elements gradually move closer to 0, indicating that the coupling modes weaken gradually. In addition, when $\omega < 0.7$, the modes with obvious negative correlation are [$C_1(C_1^{-1})$, $C_7(C_3^{-1})$], [$C_4(C_2^0)$, $C_{12}(C_4^0)$], [$C_7(C_3^{-1})$, $C_{17}(C_5^{-1})$], and [$C_{11}(C_4^{-2})$, $C_{23}(C_6^{-2})$]; in contrast, the modes [$C_1(C_1^{-1})$, $C_{17}(C_5^{-1})$], [$C_3(C_2^{-2})$, $C_{23}(C_6^{-2})$], and [$C_6(C_3^{-3})$, $C_{30}(C_7^{-3})$] have an obvious positive correlation, thereby indicating that these correlated modes have the same azimuth frequencies. According to the color bar, the lower the azimuth frequency, the higher the coupling, such as $|P_{7,17}| = 0.3123$; however, $|P_{6,16}| = 0.144$ when $\omega = 0.7$(Fig. 1). Furthermore, the color bar indicates that the coupling of positive correlated modes is weaker than that of the negative correlated modes (except autocorrelation), and thus, the study on combining positive correlated modes is ignored. We also find that the correlated modes are those with the character of 2 radial orders apart and the same azimuth frequencies, that is (C_n^m,C_{n+2}^m), $n \geqslant 1$.

The above analyses show that the wavefront of these aberration modes can be made to counteract each other in the certain concentric pupil region by utilizing the cross-coupling of Zernike modes in the concentric circle domain. This provides the theoretical basis for the study of the conjugated combination of Zernike modes.

The wavefront aberration of an actual human eye is very complex, commonly resulting in the random combination of low order aberration and a variety of higher-order aberrations. However, the influence on optical quality is not the simple sum of the role of the separate mode; thus, it is important to study the combination of Zernike mode aberrations as well as its influence on optical quality.

After combining any two Zernike mode aberrations, the RMS value increases according to Eq. (2). However, through the aberration wavefront reconstruction, the shape of some aberration wavefront becomes flat in the certain concentric pupil, and the RMS value of the corresponding region is reduced. According to the conclusion of the coupling correlation between Zernike modes

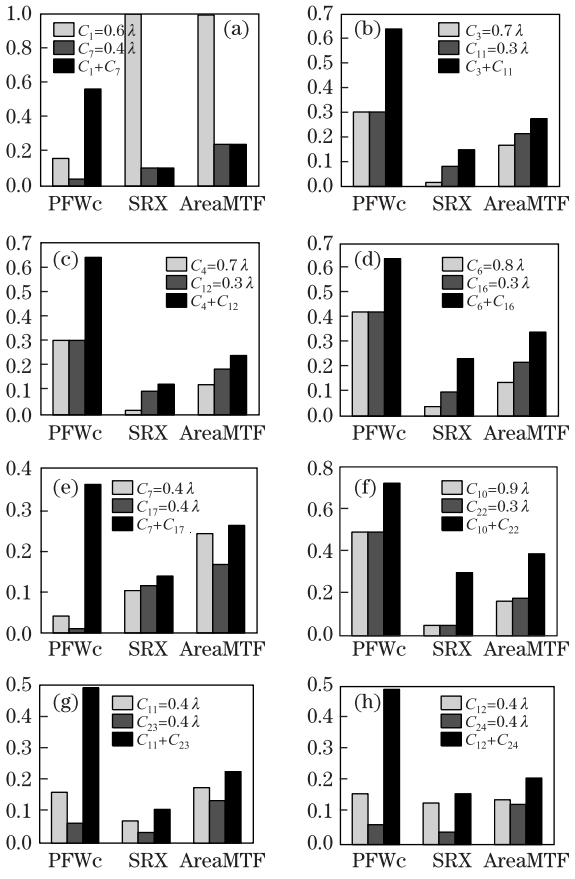

Fig. 5. Comparison of optical quality evaluation parameters before and after combining the conjugated Zernike modes.

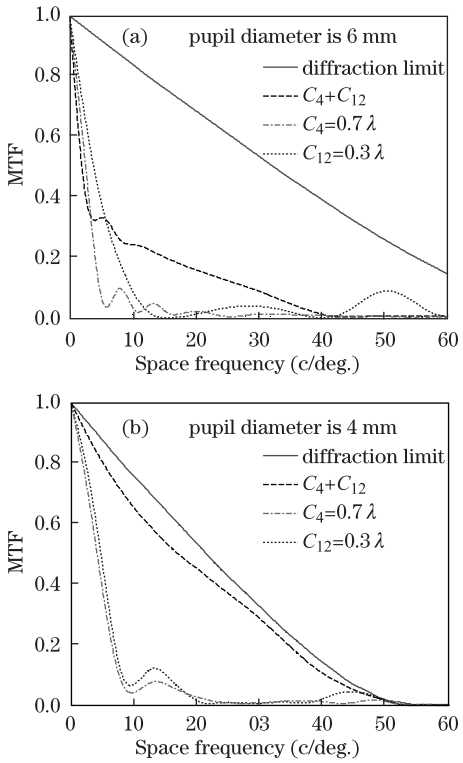

Fig. 6. MTF before and after combining the conjugated Zernike modes in (a) wavefront construction region (b) inner concentric pupil region.

discussed before, along with further research on the wavefront characteristic of Zernike mode aberration, the appearance of the abovementioned phenomenon must meet certain conditions (e.g., coupling Zernike modes with the same signs of coefficients).

Under the normal condition, the proportion of the total human eye aberration to the corresponding aberration becomes increasingly smaller with the increase in Zernike order. Therefore, this letter mainly considers the combination of the modes of orders 1 to 6 located in the left side of the central axis of the pyramid due to the symmetry of the pyramid distribution of the Zernike modes. These combined modes include $[C_n^m, C_{n+2}^m]$, $1 \leqslant n \leqslant 4$, $m \leqslant 0$, $[C_2^0(C_4), C_4^0(C_{12})]$, $[C_3^{-1}(C_7), C_5^{-1}(C_{17})]$, and so on. Wavefront aberration RMS values before and after combining these modes with the different concentric pupil diameter are shown in Fig. 2. As can be seen, the diameter of the wavefront aberration reconstruction region is 6 mm, and the concentric pupil diameter range of the evaluation is 0 to 6 mm. The figures clearly indicate that in the certain pupil region, the aberration RMS after combination is smaller than the either aberration alone, which implies that the combined modes are conjugated in the corresponding pupil region. Especially in the range of 3 to 4.5 mm in the concentric pupil diameter, all combined modes can be made to minimize the RMS. The abovementioned combination means that the wavefront shape of the combined Zernike modes has compensation and not superposition.

In order to quantitatively describe the improvement of aberration RMS due to mode combination, we define the RMS decreasing amplitude ratio R_{RMS}^p of Zernike mode combination in the certain concentric pupil region as follows:

$$R_{\mathrm{RMS}}^p = \begin{cases} 1 - \dfrac{\mathrm{RMS}_{ij}^p}{\min\left\{\mathrm{RMS}_i^p, \mathrm{RMS}_j^p\right\}} \\ \text{if } \mathrm{RMS}_{ij}^p < \min\left\{\mathrm{RMS}_i^p, \mathrm{RMS}_j^p\right\} \\ 0, \text{if other} \end{cases}. \quad (5)$$

where $p(0 \leqslant p \leqslant 6)$ is the concentric pupil diameter, RMS_i^p and RMS_j^p are the respective wavefront aberration RMS of the separate Zernike modes, and RMS_{ij}^p is the RMS after combination. Here, a bigger R_{RMS}^p value results in the improvement of the aberration at $p$mm pupil diameter after combination. The correlated Zernike modes discussed above are combined linearly with different normalized coefficients, that is, C_n^m and C_{n+2}^m are assigned from –1 to 1 with step being 0.1, respectively. The R_{RMS}^p (p=4 mm) matrices are shown in Fig. 3 in the form of gray-scale images. The horizontal and vertical coordinate scales represent the coefficients, wherein the darker the squares, the bigger the R_{RMS}^p value, and the more significant the conjugacy of the combined modes with corresponding coefficients. In contrast, the white squares stand for $R_{\mathrm{RMS}}^p = 0$, which indicates that the combination is not conjugated. We also find that the coefficients of the combined modes that meet the conjugated condition have a positive correlation. According to the darker black squares in each sub-figure in Fig. 3, the optimal linear relationships of the conjugated combination coefficients are fitted (Fig. 4), from which the formulae are obtained. For instance, the coefficient relationship of the combination modes (C_{10}, C_{22}) that meet the formula $y = 3.11x$, when $C_{22} = 0.3\lambda$, C_{10} should be about 0.9 λ, so that the maximum R_{RMS}^p can be gained.

The results above indicate that the linear conjugated combined modes are related not only to the type of mode, but also to the coefficient sign and the amount. Thus, given a couple of Zernike modes with 2 radial orders apart, with the same azimuth frequency, and the same coefficient sign and prescribed amount that satisfy the certain linear relation of distribution described in Fig. 4, the two mode aberrations can counteract each other within the certain pupil region, thereby resulting in an increasing R_{RMS}^p value.

Equation (3) also shows the independence of the Zernike modes in mathematics, and Fang *et al*. mainly discussed the influence of wavefront aberration of separate Zernike modes on optical quality[17]. However, the mathematical independence of the Zernike modes does not mean that their impact on optical quality of the optical system is independent as well. This is due to the complex aberrations of the human eye in the actual case, and the coupling effect of the Zernike modes within the different pupil region, both of which lead to a more complex optical quality. Therefore, it is necessary to study the effect of the combination, especially the conjugated combination of the Zernike mode aberrations, on optical quality.

We mainly evaluated the objective and quantitative metrics of the human eye optical quality before and after the combination of the Zernike modes. First, we chose the pairs of coefficients of the combined modes that met

the conjugated condition according to the coefficient relationship formulae shown in Fig. 4. Next, we calculated the values of PFWc, SRX, and AreaMTF, i.e., optical quality metrics introduced in Ref. [18]. The results are shown in Fig. 5. According to the results, these evaluation parameters of the combined modes are superior to the role of the separate mode, indicating that the maximization of the conjugated combined modes, except the combined modes (C_1, C_7) due to the non-influence of C_1 on optical quality, helps improve the optical quality of the system. Although there are differences in terms of the level of improvement, a consistent overall improvement of aberration is observed for the different modes.

During data processing, the increase of amplitude of the evaluation parameter after combination increases with the mode coefficient of conjugated Zernike modes, that is, the bigger the aberration, the more improvement in optical quality occurs after combination. For example, when $C_3 = 0.7\lambda$ and $C_{11} = 0.3\lambda$, after combination, the PFWc, SRX and AreaMTF values increase by 111%, 84%, and 29%, respectively, compared with the values of $C_{11} = 0.3\lambda$ alone. Moreover, when $C_3 = 1\lambda$ and $C_{11} = 0.5\lambda$, the improvements become 229%, 178%, and 51% respectively.

This sub-section presents further examination of the influence of conjugated combination on optical quality through the MTF and simulated imaging of optical system. Taking the conjugated combined modes (C_4, C_{12}) as examples, the mode coefficients are 0.7λ and 0.3λ, respectively. The MTF values before and after combination shown in Fig. 6(a) represent the distribution of MTF when the pupil is in the wavefront reconstruction region (i.e., diameter of 6 mm). The MTF of the combined modes is slightly lower than the role of the separated mode at low spatial frequency. The main reason is that the total aberration becomes larger (RMS= $\sqrt{0.7^2 + 0.3^2} = 0.76\lambda$), and the transfer ability of the low frequency information is weakened consequently. When the spatial frequency is high, especially in the frequency band of 10 to 30 c/(°), the MTF of the combined modes is obviously higher than the role of the separated mode. The main reason is that the aberration decreases when the diameter of the concentric pupil is at 4 mm (i.e., when diameter is 4 mm, RMS= 0.06λ), and when the transfer ability of the high frequency information increases. Figure 6(b) shows the distribution of MTF when the concentric pupil diameter is 4 mm. Here, we find that the improvement of MTF is much more significant, and is very close to the diffraction-limited MTF, indicating that optical quality is much better in this pupil region.

Figure 7 presents the simulated imaging results of visual target "E" before and after combining the conjugated Zernike modes. Figures 7(c) and (d) are the images at 6- and 4-mm pupil diameters, respectively, indicating a marked improvement of the imaging quality of the visual target after combination. Especially, Fig. 7(d) shows the improved resolution capability of the boundary of the visual target, thereby reaching the diffraction limited imaging result Fig. 7(e) at the 6-mm pupil diameter. The other conjugated combined Zernike modes were analyzed by adopting the above research method, allowing us to derive a consistent conclusion.

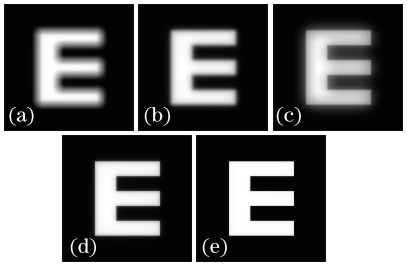

Fig. 7. Simulated imaging of the optical system before and after combining the conjugated Zernike modes. (a) C_4= 0.7 λ, (b) C_{12}= 0.3 λ, (c) C_4+C_{12} at 6 mm pupil diameter, (d) C_4+C_{12} at 4 mm pupil diameter, (e) diffraction limit at 6 mm pupil diameter.

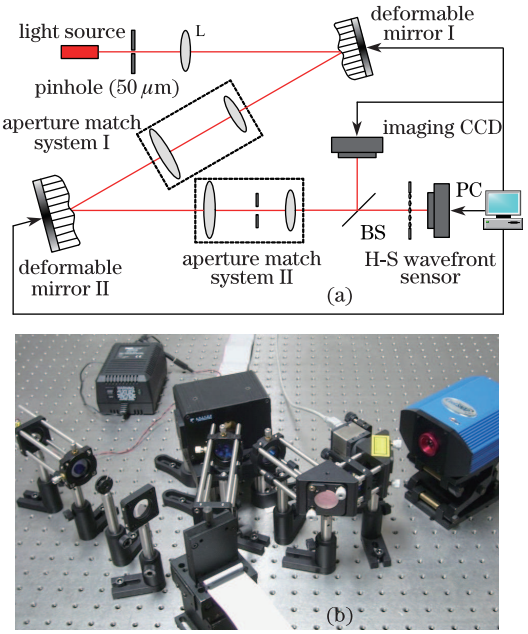

Fig. 8. Adaptive optical experimental imaging system. (a) Schematic diagram; (b) Photo. Light source, wavelength is 785 nm; pinhole, diameter is 50 μm; L, lens with focal length of 16 mm; deformable mirror I, BMC 140-channel, gold coated membrane, 8 kHz; deformable mirror II, OKO 37-channel, Al-coated membrane, 500 Hz; BS, pellicle beam splitter reflects 50% and transmits 50%; H-S wavefront sensor, 127 units, hexagonal lenslet layout, BASLER S601 camera; imaging CCD, Cool SNAP cf2.

The abovementioned discussion shows that the influence of the Zernike mode on optical quality does not have superposition, whereas for the conjugated Zernike modes, the effect of the combined modes on optical quality is represented as compensation.

We also implemented the pinhole imaging experiment based on the AO system in order to verify the feasibility and advantages of the conjugated combination of Zernike modes in fact. We set up the optical experiment platform of the imaging system. The structure schematic diagram is shown in Fig. 8. Deformable mirror I (DMI) and deformable mirror II (DMII) were used to generate and compensate aberration respectively. Among their most important characteristics introduced in Ref. [19] is the fact that DMI has higher spatial resolution than DMII. We took the conjugated combined modes (C_3 = 0.23λ,

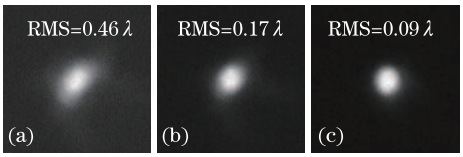

Fig. 9. Pinhole imaging results with different condition. (a) Under condition 1, residual RMS is 0.46 λ (b) under condition 2, residual RMS is 0.17 λ (c) under condition 3, residual RMS is 0.09 λ.

$C_{11} = 0.5\lambda$) for instance, we first let the DMI generate the aberration with Zernike mode $C_{11} = 0.5\lambda$. Then, we took the pinhole image with imaging CCD. The following three conditions are observed: (1) when DMII does not work, indicating that it works as a plane mirror; (2) when DMII works to generate aberration with Zernike mode $C'_{11} = -0.5\lambda$; and (3) when according to conjugated combination, DMII works to generate aberration with the Zernike mode $C_3 = 0.23\lambda$. The imaging results and residual aberration RMS of system measured with H-S wavefront sensor are shown in Fig. 9. The experiment obtains the most satisfying results under condition (3), indicating that the conjugated combination of Zernike modes has actual significance. Moreover, this conclusion is consistent with the above simulation results.

In conclusion, according to the coupling relationship between some Zernike modes over the concentric circle within the unit circle, as well as the counterbalance of the corresponding Zernike modes in the certain concentric pupil region, this letter constructs the combined Zernike modes with two radial orders apart and the same azimuth frequency. And then, according to the decreasing amplitude ratio of aberration RMS in the concentric pupil region, the linear conjugated combined Zernike modes at 4-mm concentric pupil diameter are presented. Finally, through the research on the influence of conjugated combined modes on optical quality, it is found that the optical quality of conjugated combined modes can be improved significantly after combination. It also indicates that the influence of Zernike modes' combination on optical quality does not have superposition but compensation. Of course, we do not deny the possibility of the combination of the other uncorrelated Zernike modes which will be our next research focus. Conjugated combination of Zernike modes have good application prospects in AO, such as the process of human eye aberration correction based on Zernike modes. Even more, the combination can be used in near future since the next steps in adaptive optics system technology which will use spatial light modulators that will be capable of modifying separately different areas of the pupil.

This work was supported by the Jiangsu Innovation Program for Graduate Education (No. CX10B_107Z), the Fundamental Research Funds for the Central Universities, the National High-Tech Research and Development Program of China (No. 2006AA020804), the Perspective Research Foundation of Production Study and Research Alliance of Jiangsu Province (No. BY2012009), the Project of Science and Technology Support Program of Jiangsu Province (No. BE2010652), and the Jiangsu Province Science Foundation for Youths (No. BK2012380).

References

1. J. Z. Liang, D. R. William, and D. T. Miller, J. Opt. Soc. Am. A **14,** 2884 (1997).
2. L. N. Thibos, X. Hong, A. Bradley, and R. A. Applegate, J. Vision **4,** 329 (2004).
3. L. N. Thibos, R. A. Applegate, J. T. Schwiegerling, and R. Webb, J. Refract. Surg. **18,** S652 (2002).
4. S. S. Niu, J. X. Shen, C. Liang, Y. H. Zhang, and B. M. Li, Appl. Opt. **50,** 4365 (2011).
5. J. S. Gibson, C. C. Chang, and B. L. Ellerbroe, Appl. Opt. **39,** 2525 (2000).
6. M. Lombardo and G. Lombardo, J. Cataract Refract. Surg. **36,** 313 (2010).
7. L. N. Thibos, X. Hong, A. Bradley, and X. Cheng, J. Opt. Soc. Am. A **19,** 2329 (2002).
8. R. A. Applegate, J. D. Marsack, R. Ramos, and E. J. Sarver, J. Cataract Refract. Surg. **29,** 1487 (2003).
9. L. H. Fang, W. Quan, Z. Q. Wang, and N. Ling, Opto-Electronic Engineering (in Chinese) **34,** 21 (2007).
10. L. H. Fang, X. D. He, and S. J. Li, Acta Photon. Sin. (in Chinese) **39,** 110 (2010).
11. X. Cheng, A. Bradley, S. Ravikumar, and L. N. Thibos, Optometry Vision Sci. **87,** 300 (2010).
12. Y. Benard, N. Lopez-Gil, and R. Legras, Vision Research **51,** 2471 (2011).
13. J. S. McLellan, P. M. Prieto, S. Marcos, and S. A. Burns, Vision Research **46,** 3009 (2006).
14. J. S. McLellan, S. Marcos, P. M. Prieto, and S. A. Burns, Nature **417,** 174 (2002).
15. P. de Gracia, C. Dorronsoro, E. Gambra, G. Marin, M. Hernandez, and S. Marcos, Vision Research **50,** 2008 (2010).
16. P. de Gracia, C. Dorronsoro, G. Marin, M. Hernandez, and S. Marcos, J. Vision **11,** 1 (2011).
17. L. H. Fang, Z. Q. Wang, W. Wang, and M. Liu, Acta Photon. Sin. (in Chinese) **26,** 1721 (2006).
18. J. D. Marsack, L. N. Thibos, and R. A. Applegate, J. Vision **4,** 322 (2004).
19. S. S. Niu, J. X. Shen, C. Liang, Y. H. Zhang, and B. M. Li, Spectroscopy and Spectral Analysis (in Chinese) **32,** 1795 (2012).